



## Article

# UAS Photogrammetry and TLS Technology: A Novel Approach to Predictive Maintenance in Industrial Tank Systems

Sergio García-Martos <sup>1</sup>, Pedro García-Trenza <sup>1</sup>, Antonio Saura-Campos <sup>1</sup>, Antonio Guerrero-González <sup>2,\*</sup>   
and Fernando Hidalgo-Castelo <sup>2</sup> 

<sup>1</sup> Drónica Servicios Aéreos S.L., P.I. Cabezo Beaza, Calle Berlín, 3F, Oficina 1.13, 30353 Cartagena, Spain; sergio.garcia@dronica.es (S.G.-M.); pedro.trenza@dronica.es (P.G.-T.); antonio.saura@dronica.es (A.S.-C.)

<sup>2</sup> Department of Automation, Electrical Engineering and Electronic Technology, Universidad Politécnica de Cartagena, Plaza del Hospital 1, 30202 Cartagena, Spain; fernando.hidalgo2@edu.upct.es

\* Correspondence: antonio.guerrero@upct.es

**Abstract:** This paper explores the integration of terrestrial laser scanning (TLS) and unmanned aerial system (UAS) photogrammetry for the diagnosis and evaluation of deformations in industrial tanks, demonstrating their significant contribution to preventive maintenance. TLS accurately measures distances to the tank's surface, generating detailed 3D point clouds, while UAS photogrammetry captures high-resolution images from various angles and altitudes. By combining TLS and UAS data into comprehensive 3D models, engineers can identify subtle deformations and anticipate structural failures. The study results revealed significant deviations in tank shell verticality and roundness using TLS and notable roof unevenness using UAS. Comparing 3D models before and after corrective measures showed improved structural integrity. This approach enhances safety, optimizes resources, and enables targeted interventions. The findings highlight the potential of TLS and UAS technologies to revolutionize preventive maintenance, offering an efficient, precise, and less intrusive methodology for critical infrastructure inspection. Adopting these technologies can improve safety, reduce operational risks, and optimize asset management in various industrial sectors.

**Keywords:** TLS technology; UAS photogrammetry; industrial tank inspection; structural deformation analysis; advanced inspection technologies



**Citation:** García-Martos, S.; García-Trenza, P.; Saura-Campos, A.; Guerrero-González, A.; Hidalgo-Castelo, F. UAS Photogrammetry and TLS Technology: A Novel Approach to Predictive Maintenance in Industrial Tank Systems. *Drones* **2024**, *8*, 215. <https://doi.org/10.3390/drones8060215>

Academic Editor: Fabio Remondino

Received: 5 April 2024

Revised: 17 May 2024

Accepted: 20 May 2024

Published: 22 May 2024



**Copyright:** © 2024 by the authors. Licensee MDPI, Basel, Switzerland. This article is an open access article distributed under the terms and conditions of the Creative Commons Attribution (CC BY) license (<https://creativecommons.org/licenses/by/4.0/>).

## 1. Introduction

Storage tanks play a crucial role in various industries, such as the oil, chemical, food, and power generation industries, by allowing the collection, regulation, and distribution of large volumes of liquids and gases [1]. However, due to their large dimensions, the nature of the stored products, and the operating conditions to which they are subjected, these assets are exposed to various adverse situations that cause damage or deterioration that can compromise their structural integrity and functionality [2].

Among the main damage mechanisms affecting storage tanks are corrosion, fatigue, differential settlement, overloading, buckling, and collapse [3]. These mechanisms can generate various anomalies and defects in the structure, such as geometric deviations, cracks, dents, leaks, or loss of thickness, which in turn can trigger catastrophic failures with serious consequences for the safety of people, the environment, and the continuity of facility operations [4].

To prevent and mitigate these risks, it is essential to carry out periodic inspections and evaluations of the condition of storage tanks, which allow for the timely detection and quantification of any anomalies or deviations from the planned design and operating conditions [5]. Traditionally, these inspections have been carried out manually, using conventional techniques such as visual inspection, thickness measurement by ultrasound, or leak detection by acoustic emission [6].

However, these techniques present various limitations and challenges, especially when inspecting large-scale tanks with complex geometries. On the one hand, manual inspection is usually slow, expensive, and risky for the personnel involved, as it requires direct access to the structure, often at height and in hazardous environments [7]. On the other hand, conventional techniques only allow for obtaining specific and localized information about the state of the tank, which makes it difficult to detect and evaluate global or progressive anomalies, such as geometric deviations or differential settlements [8].

In recent decades, various advanced structural inspection and monitoring techniques have been developed based on sensors and emerging technologies, which seek to overcome the limitations of traditional methods and improve the efficiency, safety, and reliability of industrial asset structural integrity management [9]. Among these techniques, terrestrial laser scanning (TLS) and photogrammetry with unmanned aerial systems (UAS) stand out, which allow the complete geometry of the structure to be captured quickly, safely, and in detail, generating high-resolution and precision three-dimensional digital models [10].

Terrestrial laser scanning (TLS) is an active remote sensing technique that employs a laser device to emit a beam of light and determine the distance to an object's surface by analyzing either the time of flight of the reflected pulses or the phase difference between the emitted and received signals. Specifically, the Faro Focus S-150 laser scanner employed in this study utilizes phase-shift measurement technology, which allows for obtaining a high point density and sub-millimeter accuracy within a working range of up to 150 m [11]. By combining distance and angle measurements for each laser pulse, the scanner generates a three-dimensional point cloud that represents the geometry of the scanned object with millimeter precision [12]. This technique has been widely used in industry for the as-built documentation and dimensional control of structures and equipment, including storage tanks [13].

UAS photogrammetry, on the other hand, is a passive measurement technique that uses aerial images acquired with unmanned aerial systems (UAS) to reconstruct the three-dimensional geometry of an object or scene using computer vision algorithms and bundle adjustment [14]. Unlike TLS technology, which directly captures the 3D coordinates of points, UAS photogrammetry generates a point cloud by identifying and correlating common features in multiple overlapping images [15]. This technique has experienced a significant boom in recent years thanks to advances in drone technology and its ability to capture information from large areas quickly and economically [16].

Despite its great potential, the application of TLS technology and UAS photogrammetry techniques for the inspection of storage tanks is still a nascent field of research and development, which presents various challenges and opportunities for improvement [17]. On the one hand, methodologies and standards are required that allow for the integration and maximum utilization of the information generated by these techniques in asset integrity and maintenance management processes [18]. On the other hand, advanced point cloud processing and analysis tools and algorithms are needed that allow for the efficient and reliable extraction of the relevant parameters and indicators for evaluating the condition and behavior of tanks [19].

In this context, the present study aims to contribute to the advancement in the application of TLS technology and UAS photogrammetry techniques for the inspection and evaluation of storage tanks through the development and validation of a comprehensive methodology that allows taking full advantage of the potential of these technologies to improve the safety, reliability, and efficiency of these critical assets.

To this end, a large fuel storage tank has been selected as a case study for analyzing signs of deterioration and geometric anomalies. A three-dimensional measurement campaign for the tank was carried out using a high-precision terrestrial laser scanner and a drone equipped with a high-resolution camera. The point clouds generated by both techniques were processed, aligned, and merged to generate a complete and detailed three-dimensional model of the tank.

Using this model, various geometric and structural analyses have been conducted, including the evaluation of the verticality and roundness of the shell, the flatness of the bottom and roof, the detection of local anomalies such as dents, buckling, or corrosion, and the comparison with design data and regulatory tolerances. Additionally, the three-dimensional model has been integrated with other relevant data, such as previous inspection and repair history, process and operation data, and finite element models, to perform a comprehensive assessment of the tank's condition and behavior.

The results obtained have made it possible to identify and quantify various geometric deviations and structural anomalies in the tank, some of which exceed the tolerances established by applicable standards, such as API 650 for the design and construction of welded storage tanks. Furthermore, deformation and deterioration patterns have been detected that suggest the existence of active damage mechanisms, such as differential ground settlement, internal corrosion, or compression buckling.

Based on these findings, specific recommendations have been made for the repair, reinforcement, and maintenance of the tank, as well as for the improvement of future inspection and evaluation procedures. Likewise, opportunities for improvement and future lines of research have been identified to continue advancing the application of three-dimensional measurement techniques in the integrity management of storage tanks and other industrial assets.

Among the main conclusions of the study, it is highlighted that the combination of TLS technology and UAS photogrammetry techniques allows for the generation of high-resolution and precise three-dimensional models of storage tanks, which facilitate the detection and quantification of anomalies and geometric deviations that can compromise their structural integrity and functionality. Furthermore, the importance of integrating these models with other relevant sources of information, such as design data, inspection and maintenance histories, and numerical models, is emphasized to make more comprehensive and reliable assessments of tank condition and performance.

Moreover, it is concluded that the methodology developed in this study represents a significant advance in the application of advanced three-dimensional measurement techniques for the inspection and evaluation of storage tanks by providing a systematic and validated approach to fully exploit the potential of these technologies in managing the integrity of these critical assets. However, it is recognized that there are still various challenges and opportunities for improvement in this field that require continuous research, development, and innovation efforts.

The following sections of the article present the developed methodology and the obtained results in detail, as well as a discussion of them in the context of the state-of-the-art and practical implications for the industry. Finally, the conclusions and recommendations derived from the study are presented, along with perspectives for future work in this field.

## 2. Materials and Methods

The object of study in this work is a vertical cylindrical carbon steel industrial tank with dimensions of 29,120 mm in diameter and 26,320 mm in height, composed of 11 shell courses, each measuring 2391 mm in height. The tank is designed according to the API 650 standard for fuel storage and has a nominal capacity of 9357 m<sup>3</sup>. Figure 1 shows an exterior view of the studied tank.

To conduct the dimensional analysis of the tank, the equipment used is described in the following sections.



**Figure 1.** Exterior view of the vertical storage tank studied in this work.

### 2.1. FARO Focus S-150 Terrestrial Laser Scanner

A FARO Focus S-150 terrestrial laser scanner was used to capture the geometry of the tank's shell and base. This device employs phase-shift measurement technology and performs up to 976,000 point measurements per second, generating a high-density three-dimensional point cloud.

The Focus S-150 has a maximum range of 150 m and an accuracy of  $\pm 1$  mm at 25 m. It features an integrated 4-megapixel color camera to capture images that allow for colorizing the point cloud. The vertical field of view is  $300^\circ$ , and the horizontal field of view is  $360^\circ$ , with an angular resolution of  $0.009^\circ$  and a point size of 2.25 mm at 10 m.

The scanner has compact dimensions ( $230 \times 183 \times 103$  mm) and weighs only 4.2 kg, which facilitates its transportation and handling in the field. Furthermore, it is equipped with a dual-axis compensator, electronic compass, altimeter, and integrated GPS for automatic georeferencing of the scans. These features enable the scanner to capture accurate and detailed 3D data of the tank's geometry, even in challenging field conditions. The high point density and sub-millimeter accuracy provided by the Focus S-150 allow for a comprehensive analysis of the tank's shell and base, facilitating the detection of any deformations, irregularities, or structural issues that may require attention.

### 2.2. DJI Mavic 2 Pro Drone with Hasselblad Camera

A DJI Mavic 2 Pro drone equipped with a Hasselblad L1D-20c camera was used to inspect the tank roof. This camera features a 1-inch CMOS sensor with 20 effective megapixels, enabling the capture of high-resolution images. The lens has a focal length equivalent to 28 mm in 35 mm format and an adjustable aperture from  $f/2.8$  to  $f/11$ , with autofocus capabilities from 1 m to infinity. The camera offers a wide ISO range of 100 to 12,800 (100–6400 for video) and a shutter speed range of 8 s to  $1/8000$  s, allowing for adaptability to various lighting conditions. Furthermore, it can capture still images in both JPEG and DNG (RAW) formats with a maximum size of  $5472 \times 3648$  pixels and provides various photography modes such as single shot, burst, automatic exposure bracketing (AEB), and panorama. Exposure control can be set to automatic or manual, and white balance options include automatic, sunny, cloudy, incandescent, and fluorescent. The camera is mounted on a 3-axis gimbal stabilizer, which enables precise control of tilt, roll, and pan, ensuring sharp and stable images during the tank roof inspection.

The use of the DJI Mavic 2 Pro drone with the Hasselblad L1D-20c camera offers several advantages for tank roof inspections. The high-resolution sensor and adjustable aperture allow for detailed image capture, even in challenging lighting conditions. The autofocus capabilities ensure that the images remain sharp across a wide range of distances, while the various photography modes provide flexibility in capturing different types of



shots. The 3-axis gimbal stabilizer is crucial for maintaining image stability and clarity, especially when operating the drone in windy conditions or at higher altitudes. The compact size and advanced features of this drone–camera combination make it an efficient and effective tool for conducting comprehensive visual inspections of tank roofs, enabling the identification of potential issues such as cracks, corrosion, or structural deformations.

### 2.3. Software

The processing of the captured data was carried out using the following specialized software:

- **FARO SCENE:** This software was used for managing and preprocessing the laser scanner data. It allows for the merging of individual scans, application of filters, and export of point clouds in different formats. SCENE enables the efficient handling and optimization of large point cloud datasets obtained from the FARO Focus S-150 terrestrial laser scanner.
- **Pix4Dmapper:** This photogrammetry software was employed for processing the aerial images captured by the drone. It generates orthomosaics, digital surface models, and dense point clouds from the input images. Pix4Dmapper was used to create a three-dimensional point cloud of the tank roof, providing detailed geometric information for further analysis.
- **BuildIT Construction:** This specialized software for 3D point cloud analysis in architecture, engineering, and construction applications was employed for detecting geometric deviations in the tank structure. BuildIT Construction provides advanced tools for evaluating the verticality and roundness of the tank shell, enabling the identification of potential structural issues or deformations.
- **3DReshaper:** This software was used for processing and analyzing the irregular triangular meshes generated from the point clouds. 3DReshaper allows for the editing, repairing, and inspection of 3D meshes, making it suitable for assessing the flatness of the tank roof. By comparing the generated mesh with a reference plane, deviations and irregularities in the roof structure can be identified and quantified.

The combination of these specialized software packages forms a comprehensive workflow for processing and analyzing the data captured by TLS technology and UAS photogrammetry. Each software package contributes to a specific aspect of the data processing pipeline, from preprocessing and point cloud generation to alignment, fusion, and geometric analysis. The use of these tools enables the extraction of valuable information about the tank's structural condition, facilitating the identification of potential issues and supporting informed decision making for maintenance and repair strategies.

### 2.4. Methodology

This section provides a detailed description of the procedures and methods employed during the different stages of the study, including the preliminary phase, field work phase, data preprocessing phase, and data processing phase.

In the preliminary phase, initial estimations and considerations were made to define the study parameters and objectives. All available technical documentation of the tank under study was reviewed, including plans, specifications, and any other relevant information. Based on this documentary analysis, the technical and logistical requirements necessary to carry out the field work effectively and efficiently were established.

During the field work phase, on-site data collection was performed using the drone and TLS equipment mentioned in the previous section. The environmental conditions and any other relevant variables that could influence the results were meticulously recorded.

After data acquisition, a preprocessing phase was conducted to prepare the obtained data. In this stage, individual TLS scans were merged into a single point cloud, applying filtering techniques to remove noise and outliers. Additionally, the images captured by the drone were processed to generate a dense point cloud and a 3D model of the tank surface.

Subsequently, in the data processing phase, analysis and modeling techniques were applied to extract meaningful information from the preprocessed data. The specialized software described previously was used to process and visualize the results, integrating the point clouds from the TLS and drone. A thorough quality control process was carried out to ensure the integrity and reliability of the processed data.

By following this structured methodology, this study aims to obtain accurate and comprehensive data on the tank's geometric characteristics and structural condition. The combination of advanced data acquisition techniques, such as TLS and UAS photogrammetry, along with rigorous preprocessing and processing procedures, enables the detection and assessment of potential deformations, irregularities, or other issues that may affect the tank's integrity and performance. The results obtained from this analysis provide valuable insights for decision making regarding maintenance, repair, or rehabilitation strategies for the storage tank under study.

#### 2.4.1. Field Work Phase with TLS

To obtain a detailed three-dimensional model of the storage tank, high-resolution terrestrial laser scanning (TLS) was performed using 28 scanning positions around the tank's external envelope, covering the entire outer surface from the base to the roof. The location of each scan is shown in Figure 2, where the blue points represent the laser positions. The thicker blue points indicate multiple scanning locations in close proximity to each other. In order to capture the most information from the elevated areas of the tank, the TLS was positioned on the helical staircase surrounding the structure.

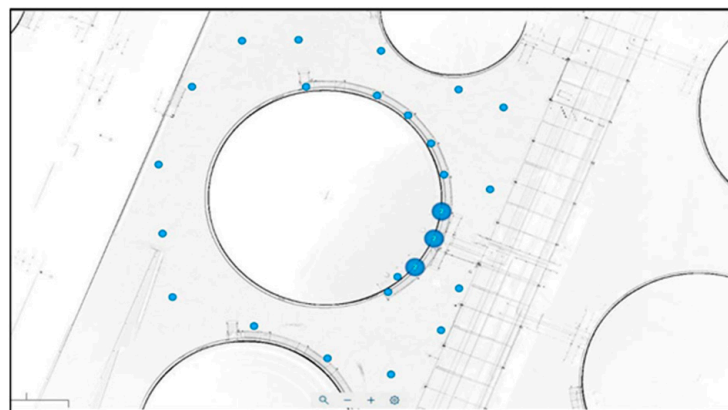


**Figure 2.** Locations of the 28 laser scans (blue points) around the tank.

An angular resolution was used that allowed for obtaining a sufficiently dense point cloud to conduct a comprehensive study of the tank's envelope, seeking a high level of detail. In total, 58 million points were captured with an accuracy of  $\pm 1$  mm and an adequate spatial resolution to provide an accurate representation of the geometry and current condition of the storage tank.

The total duration of the field work for laser scanning was 6 h, including equipment setup time, data acquisition, and travel between scanning positions. There were no significant interruptions during the process, and the weather conditions were favorable, with clear skies and a moderate wind.

#### 2.4.2. Field Work Phase with UAS

To obtain a complete point cloud of the tank roof, a photogrammetric survey was conducted using a programmed flight with the DJI Mavic 2 Pro drone. An automated flight route was designed using the DroneDeploy software, planning the route in a grid pattern over the study area and programming the drone to fly at an altitude of 60 m above ground level and at a speed of 5 m/s.

A total of 250 images were captured with a frontal (frontlap) and lateral (sidelap) overlap of 70% and a spatial resolution (GSD, ground sampling distance) of 0.8 cm/pixel. The total flight time was 25 min, divided into two battery cycles to cover the entire roof. Additionally, 10 oblique images were taken from different angles to improve the geometry of the photogrammetric reconstruction.

The main objective was to capture images of the tank from all possible perspectives, ensuring comprehensive coverage of the structure. The flight parameters and camera settings were carefully adjusted to ensure the quality and detail of the captured images. The lighting conditions were optimal, with indirect sunlight and no pronounced shadows on the roof.

Through this automated flight strategy, the upper part of the tank was successfully photographed from multiple perspectives, laying the foundation for generating a complete and accurate point cloud of the roof.

#### 2.4.3. TLS Data Preparation Phase

The data captured by the TLS during the field work requires further processing to obtain an accurate and coherent point cloud of the tank's envelope. This processing was carried out using FARO's specialized software, SCENE, which allows for the merging and adjustment of individual scans to generate a complete three-dimensional model.

The preprocessing of the 28 individual laser scans was performed in FARO's SCENE software. The following filters and operations were applied to obtain a point cloud in the best condition for subsequent study: dark point filter, isolated point filter, and redundant point filter.

After field capture and the application of the aforementioned filters, a refined point cloud of 52 million points was obtained, with a file size of 8.5 GB in .e57 format. The unified point cloud of the tank was initially exported in SCENE's native format and subsequently converted to the widely used .e57 format for point cloud exchange, which exports the individual point clouds of each scan already located in their correct position.

Through precise registration of the scans and the application of filtering techniques, a unified and coherent point cloud of the tank's envelope was obtained. The three-dimensional model generated in SCENE served as the basis for subsequent analyses and evaluation of the structure's geometry and condition.

For point cloud analysis and dimensional control of the tank, FARO's BuildIT Construction software was used. This program was employed to analyze and detect possible deformations in the tank structure based on the data obtained through the laser scanner.

Initially, point clouds in .e57 format are imported and merged to obtain a single comprehensive point cloud representation of the tank. Subsequently, the coordinate axis is positioned at the base of the tank to facilitate the placement of horizontal sections. The ground point cloud, essential for defining the tank's geometry, is then extracted. A plane is created to represent the ground's flatness, and the tank's ideal cylindrical geometry is defined for analysis purposes. Finally, a reference point is established using an easily identifiable feature, such as a manhole on the tank wall, to serve as a reference for vertical sectioning. Figure 3 illustrates the key elements and reference systems used in the BuildIT Construction software for analyzing the tank's geometry based on laser scanner data. Figure 3 showcases the ground point cloud, ground plane, real and ideal cylinders, coordinate system (X, Y, Z), and the clocking point. These elements serve as essential components for defining the tank's base, orientation, and reference geometry.

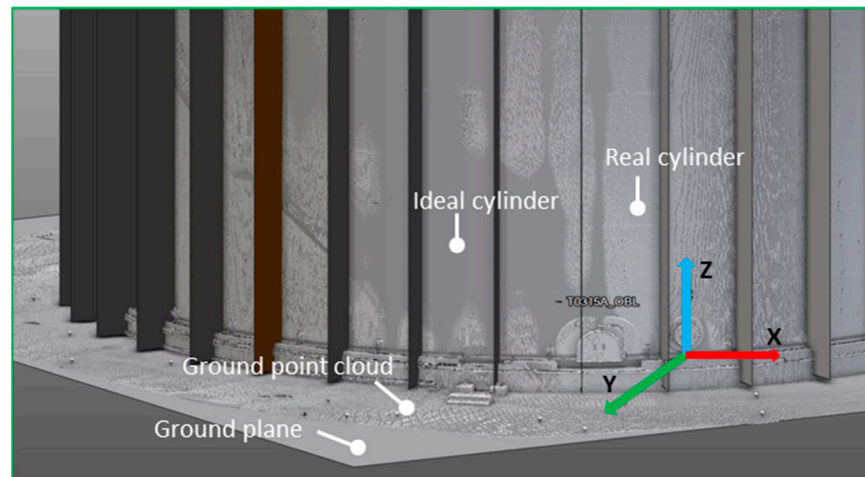


**Figure 3.** Point cloud, ground plane, ideal cylinder, and reference systems.

### 2.5. Data Processing de las Nubes de Datos del TLS

After completing the initial configuration and defining the reference geometry, a detailed analysis of the tank was carried out by generating multiple horizontal and vertical sections.

For the detailed analysis of the tank, it is crucial to carefully define the location and height of the horizontal sections. When placing these cuts, special attention should be paid to avoid coinciding with the welds or being close to them, as these areas can introduce distortions in the measurements. The definition of the horizontal sections is performed by defining cutting points at the desired heights, using their exact location with respect to the previously established custom coordinate system. It is essential that these points are strategically placed, ensuring that they do not overlap with welds or are too close to them. Once the points are created, the horizontal sections passing through these previously created points must be generated (Figure 4). A total of 33 horizontal sections were created, providing a detailed view of the tank's geometry at different heights and allowing for the evaluation of deviations from the ideal shape.



**Figure 4.** Horizontal and vertical sections of the studied tank.

To conduct a detailed analysis of the tank, it was decided to divide it into 36 radial vertical sections, resulting in a separation of 10 degrees between each section. It is important to note that section 1 is located approximately 2 degrees to the left of the 0-degree reference point of the tank's general layout plane.

Once all the previous steps are completed and the horizontal and vertical sections are defined, the configuration illustrated in Figure 4 is obtained. A total of 1188 cylindrical sectors were defined, delimited by the 33 horizontal sections or heights and 36 radial vertical sections. As an example, the reference sections are highlighted in yellow: horizontal section 1 (with a height of 25,976 mm) and vertical section 1 (corresponding to 0 degrees).

The combination of horizontal and vertical sections enables a comprehensive analysis of the tank's geometry, offering a detailed perspective on its shape and potential deviations at various heights and angular positions. This systematic approach establishes a foundation for the accurate assessment of the tank's structural integrity and the identification of areas that may necessitate attention or intervention.

Once the sections are prepared and the analysis parameters are defined according to current regulations, a detailed analysis of the tank's geometry is carried out. The results obtained from the analysis allow for the evaluation of the tank's structural integrity and the identification of possible deviations that require attention or intervention. This systematic methodology, based on current regulations, ensures a rigorous and objective assessment of the tank's condition, providing valuable information for decision making regarding its maintenance and safety.

#### *2.6. Photogrammetric Processing of Roof Images Captured by Drone*

The images of the tank roof captured by the drone were processed using Pix4Dmapper software, following the standard workflow for UAS photogrammetry projects. The process included the automatic orientation of the images by identifying homologous points between them, which allows for establishing the spatial relationships between the different takes, and the measurement of ground control points using a GNSS (global navigation satellite system) technology with RTK (real-time kinematic) correction for direct georeferencing of the image block captured by the drone. These points provide a precise reference to adjust and scale the photogrammetric model.

In this study, a photogrammetric survey was conducted to generate a high-resolution dense point cloud of a 900 m<sup>2</sup> area using Pix4Dmapper software. A total of 250 images were captured with a frontal (frontlap) and lateral (sidelap) overlap of 70% and a spatial resolution (GSD, ground sampling distance) of 0.8 cm/pixel. For this purpose, a grid flight was conducted over the tank cover, sweeping an area of 30 × 30 m.

The captured images were processed using Pix4Dmapper version 4.7.5 on a high-performance computer equipped with an Intel Core i9-10900K processor, 64 GB of RAM, and an NVIDIA RTX 3080 graphics card. The photogrammetric processing workflow included point cloud densification, which resulted in a total of 21,260,071 densified 3D points, with an average density of 23,600 points/m<sup>3</sup>. This high-density point cloud provides a detailed and accurate representation of the surveyed area, enabling precise measurements, analysis, and visualization of the captured geometry. This high-density point cloud, shown in Figure 5, provides a detailed and accurate representation of the surveyed area, enabling precise measurements, analysis, and visualization of the captured geometry. The processing time for the point cloud generation was 2 h, leveraging the computational power of the specified hardware configuration.

The described results were obtained by adjusting various parameters within the software's processing options. The image matching process was performed using a grid flight algorithm and geometrically verified matching. The camera calibration involved optimizing the camera parameters, giving high priority to the internal parameters. Once this initial image alignment processing was completed, the point cloud creation was carried out. For the densification of the point cloud, the image scale was set to full, and a minimum of 3 matches were required.



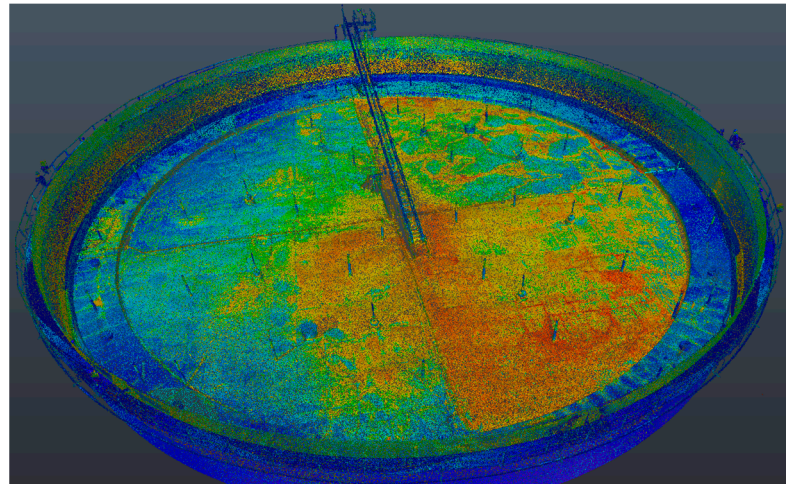


**Figure 5.** Dense point cloud of the tank roof.

The grid flight algorithm employed in the image matching process ensures a systematic and comprehensive coverage of the surveyed area, enhancing the reliability and completeness of the resulting point cloud. By utilizing geometrically verified matching, the software validates the spatial consistency of the matched features, minimizing the impact of outliers and improving the overall accuracy of the alignment process.

During camera calibration, the optimization of camera parameters, with a focus on the internal parameters, is crucial for achieving accurate 3D-reconstruction results. The internal parameters, such as focal length, principal point, and lens distortion coefficients, directly influence the geometric accuracy of the derived point cloud. By giving high priority to these parameters, the software can effectively minimize potential distortions and ensure a more precise representation of the captured scene.

The densification of the point cloud is a critical step in generating a detailed and comprehensive 3D model. By setting the image scale to full, the software utilizes the maximum available resolution of the input images, preserving fine details and enabling the creation of a high-density point cloud. The requirement of a minimum of 3 matches per point ensures the robustness and reliability of the densification process, as each point is supported by multiple observations from different images, reducing the impact of noise and outliers.

The combination of these processing parameters, including the grid flight algorithm, geometrically verified matching, camera parameter optimization, full image scale, and minimum match requirement, contributes to the generation of a high-quality and accurate point cloud.

The analysis of the tank roof point cloud is performed using 3DReshaper software. The process involves importing the cloud in .e57 format, cleaning unnecessary parts, creating a mesh from the triangulation of the points, generating a horizontal reference plane, and automatically comparing the mesh with said plane.

The mesh model is a triangulated representation of the point cloud, where points are connected to form a solid or closed structure. The creation of the mesh involves adjusting parameters such as the average distance between points and the size of the triangles to achieve the best possible representation of the object's surface. If there is incomplete information in the point cloud, the mesh is completed through numerical calculation and indicated in blue areas, as shown in Figure 6.

In this study, a high-quality triangular mesh model was generated from a dense point cloud using 3DReshaper software, as illustrated in Figure 6. The input data were obtained from a previous photogrammetric survey and consisted of 21,260,071 points with an average spacing of 0.8 cm.

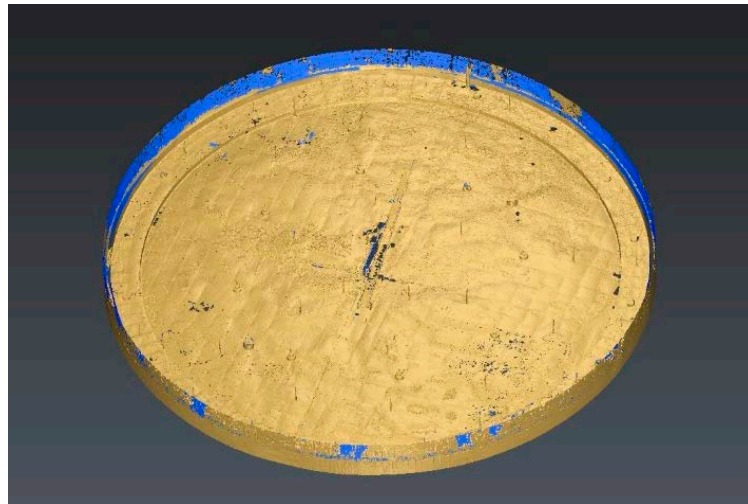


**Figure 6.** Tank roof mesh model.

The mesh generation process was performed with a set of parameters optimized for quality and efficiency. For the creation of the mesh itself, the following values were specified: Regarding noise reduction, a normal sampling was performed with an average distance between points of 0.161638 cm. On the other hand, a triangle size of 0.484915 was established for hole detection. The mesh generation process took 1 h and 30 min to complete, resulting in a mesh composed of 28,125,000 triangles and 14,062,500 vertices. The average triangle edge length of 1.6 cm demonstrates the high level of detail captured in the mesh model. The mesh covers a surface area of 899.8 m<sup>2</sup>, accurately representing the spatial extent and dimensionality of the studied area.

A mesh quality analysis was conducted to assess the geometric properties and integrity of the generated mesh. The minimum triangle angle was found to be 15 degrees, while the maximum angle was 120 degrees, indicating a well-structured and balanced triangulation. The average triangle aspect ratio of 1.5 suggests a good proportionality between the triangle edges, with 95% of triangles having an aspect ratio below 2 and 99% below 3, further confirming the mesh's quality.

To optimize the mesh for downstream applications, additional processing steps were performed. Mesh simplification was applied to reduce the triangle count to 25% of the original mesh, resulting in a simplified mesh with 7,031,250 triangles. This simplification process took 20 min to complete and yielded a file size of 425 MB, significantly reducing the storage requirements while preserving the essential geometric features.

Laplacian smoothing, a commonly used algorithm for mesh refinement, was applied with 3 iterations to further enhance the mesh's visual appearance and smoothness. This smoothing process took 10 min to complete and improved the overall aesthetic quality of the mesh.

To analyze the flatness of the tank roof, a completely horizontal reference plane was created and a comparison between the roof mesh and this plane was performed (Figure 7). The results of this comparison reveal the deviations between the roof mesh and the reference plane, enabling the visualization and quantification of deformations or irregularities in the roof structure.

The analysis of the roof flatness, in conjunction with the examination of the tank envelope, provides a comprehensive evaluation of the structure's overall condition. This information facilitates informed decision making regarding maintenance, repair, or intervention strategies necessary to ensure the tank's integrity and operational safety.

The photogrammetric processing of the images captured by the drone enables the generation of an accurate and detailed representation of the tank roof geometry. The resulting point cloud complements the data acquired by the terrestrial laser scanner, providing complete coverage of the tank structure. By combining both datasets, a comprehensive

analysis of the tank's geometry and condition can be conducted, taking into account both the envelope and the roof.

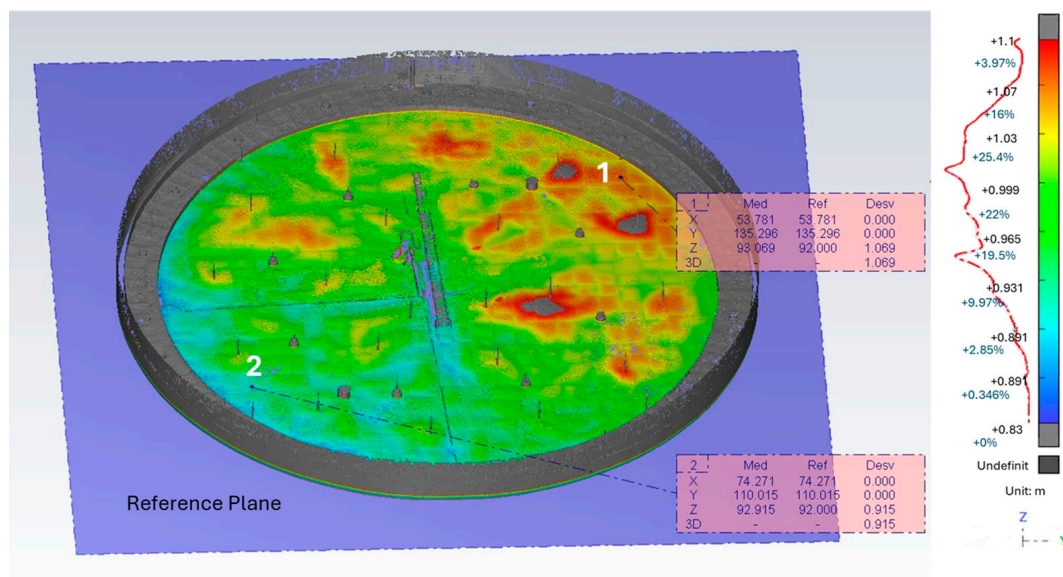


**Figure 7.** Comparison of the mesh with the reference plane.

### 2.7. Applicable Regulations

The design and manufacture of storage tanks are governed by various standards that establish the allowable tolerances for their geometric characteristics. In the case of the tank under study, the relevant standards are API 650 (Welded Tanks for Oil Storage) and API 653 (Tank Inspection, Repair, Alteration, and Reconstruction).

API 650, which focuses on the construction of welded tanks for oil storage, specifies a roundness tolerance of  $\pm 19$  mm for tanks with diameters between 12 and 45 m. This tolerance is measured at a distance less than or equal to one foot from the shell-to-bottom weld. Additionally, API 650 establishes a maximum verticality tolerance of  $1/200$  of the total height of the tank. For the tank in this study, which has a height of 26.320 m, the maximum allowable verticality deviation would be 132 mm.

On the other hand, API 653, which deals with the inspection, repair, alteration, and reconstruction of tanks, specifies a roundness tolerance of  $\pm 19$  mm for tanks with diameters between 12 and 45 m, measured at a distance equal to or less than 1 foot (approximately 30 cm) above the shell-to-bottom joint. For measurements taken more than 1 foot above the bottom joint, the radius tolerance should not exceed  $\pm 57$  mm. Furthermore, API 653 sets a maximum verticality tolerance of  $1/100$  of the tank height, with an absolute maximum of 127 mm.

When comparing both standards, it becomes evident that API 653 is more restrictive in terms of vertical and roundness tolerances. Consequently, for the purposes of this study, the criteria mentioned in API 653 will be applied to evaluate the geometric characteristics of the tank under investigation. By adhering to these stricter tolerances, a more rigorous assessment of the tank's structural integrity can be achieved, ensuring compliance with the highest industry standards for inspection and maintenance.

### 3. Results

In this section, the results of the studies conducted to evaluate the verticality and roundness of the tank shell, as well as the horizontality of the roof, are presented. The analysis of the tank shell is approached through three different perspectives: roundness analysis, which allows examining the tank's geometry at different heights; verticality analysis, which provides information about the structure's verticality; and wall analysis (2D map), which offers a global view of the deviations and deformations present on the tank's surface. The

results obtained through these analyses are detailed below, providing a comprehensive evaluation of the tank's geometric integrity and allowing for the identification of possible areas that may require attention or intervention.

### 3.1. Analysis of the Tank Shell

The average deviation of all tank sectors is  $-1.628$  mm, indicating a slight inward deviation that could be considered insignificant. However, it is important to highlight the most pronounced deviations both towards the exterior and the interior of the tank, as these can have a significant impact on its structural integrity.

Table 1 shows the tank sectors with the most pronounced deviations towards the exterior, identified through the height and orientation according to the horizontal and vertical sections defined in the methodology. The maximum deviation towards the exterior is found in section 28, at a height of 3.615 mm and an orientation of  $220^\circ$ , with a value of 82.094 mm. Other significant deviations towards the exterior are observed in sections 27, 29, 28, and 26, with values ranging between 72.199 mm and 79.261 mm.

**Table 1.** Maximum outward deviations in the tank.

Section	Height (mm)	Orientation ( $^\circ$ )	Deviation (mm)
28	3.615	$220^\circ$	82.094
27	4.437	$220^\circ$	79.261
29	2.883	$200^\circ$	77.123
28	3.615	$210^\circ$	74.653
26	5.284	$220^\circ$	72.199

On the other hand, Table 2 presents the tank sectors with the largest deviations towards the interior. The largest deviation is found in section 15, at a height of 13.953 mm and an orientation of  $20^\circ$ , with a value of  $-94.840$  mm. Other significant deviations towards the interior are observed in sections 16, 13, 1, and 14, with values varying between  $-86.386$  mm and  $-92.133$  mm.

**Table 2.** Minimum inward deviations in the tank.

Section	Height (mm)	Orientation ( $^\circ$ )	Deviation (mm)
15	13.953	$20^\circ$	$-94.840$
16	13.131	$20^\circ$	$-92.133$
13	15.526	$20^\circ$	$-90.278$
1	25.976	$50^\circ$	$-88.276$
14	14.809	$20^\circ$	$-86.386$

#### 3.1.1. Tank Roundness Analysis

The roundness analysis of the tank sections revealed several deviations that exceed the tolerances specified in API 653. The standard sets a roundness tolerance of  $\pm 19$  mm for tanks with diameters between 12 and 45 m, measured at a distance equal to or less than 1 foot (approximately 30 cm) above the shell-to-bottom joint. For measurements taken more than 1 foot above the bottom joint, the radius tolerance should not exceed  $\pm 57$  mm.

Table 3 presents the most significant deviations identified in this study. It is crucial to highlight that several sections exhibit deviations that surpass the allowable limits.

**Table 3.** Deviations in tank horizontal sections.

Section	Height (mm)	Maximum (mm)	Minimum (mm)	Difference (Max-Min) (mm)	Mean
15	13.953	42.963	−94.840	137.803	−12.517
33	254	31.576	−25.736	57.312	1.021
01	25.976	31.635	−88.276	119.911	−24.482
22	8.402	55.660	−43.811	135.909	−0.491
27	4.437	79.261	−56.648	135.909	3.634

In section 33, both the outward and inward deviations exceed the allowable limits specified by the API 653 standard for the height of 254 mm. According to the standard, the roundness tolerance at this height should be within  $\pm 19$  mm. It is important to note that section 33 contains a significant amount of tank instrumentation, which could be a contributing factor to these deviations. Given that the deviations in this section are significant according to the standard, corrective measures should be implemented to address these issues.

Section 27 exhibits a maximum outward deviation of 79.261 mm, which surpasses the allowable limit of  $\pm 57$  mm specified in the API 653 standard for the corresponding height. This excessive deviation indicates a substantial departure from the ideal circular shape and warrants further investigation and potential remedial actions.

Sections 15 and 01 demonstrate maximum inward deviations of  $-94.840$  mm and  $-88.276$  mm, respectively. These values significantly exceed the allowable limit of  $-57$  mm specified in the API 653 standard for the corresponding heights. Such excessive inward deviations suggest the presence of underlying structural issues that require immediate attention and corrective measures.

Furthermore, section 01 exhibits the highest mean deviation in absolute value ( $-24.482$  mm), indicating a general tendency towards the tank's interior in this section. This suggests that the walls of section 01 may be experiencing inward deformation, which could be caused by factors such as structural weaknesses. In contrast, section 22 shows the lowest absolute mean value ( $-0.491$  mm), suggesting greater uniformity in the roundness of this section. This indicates that section 22 has a more consistent and evenly distributed shape, with minimal deviations from the ideal circular profile.

Section 27 also deserves special attention due to the significant difference between its maximum outward and inward deviation values (135.909 mm), with a maximum outward value of 79.261 mm and a maximum inward value of  $-56.648$  mm. These deviations indicate a considerable lack of roundness in this section, which may be attributed to localized factors such as foundation settlement, thermal stresses, or fabrication issues.

The excessive deviations observed in sections 33, 27, 01, and 15 highlight significant departures from the ideal circular shape and may be indicative of underlying structural issues. The large differences between the maximum outward and inward deviation values in these sections further emphasize the severity of the roundness irregularities and the need for prompt action.

When analyzing all horizontal sections, it was detected that sections 1, 2, 3, 8, 9, 10, 11, 12, 13, 14, and 15 have values lower than  $-57$  mm, indicating significant inward deviations. On the other hand, rows 25, 26, 27, 28, and 29 have values greater than 57 mm, suggesting substantial outward deviations. Row 28 exhibits the highest value of 82.094 mm. These excessive deviations, both inward and outward, raise concerns about the structural integrity of the tank and its compliance with industry standards. Immediate attention and corrective measures are necessary to address these issues and ensure the safe operation of the storage facility. Further investigation into the causes of these deviations and a comprehensive assessment of the tank's condition are recommended to develop an appropriate maintenance and repair plan.



Figure 8 indicates that horizontal section 15 of the tank presents a significant lack of roundness, with a wide variation between the maximum outward and inward deviations (137.803 mm) that is the largest among all the analyzed sections. The graph shows an asymmetric distribution of deviations, with a predominantly negative zone between 0° and 180° and a positive one between 180° and 360°, resulting in an oval shape. This lack of uniform roundness suggests structural problems that could be due to imperfections in construction, uneven loads, ground settlements, welding issues, or damage during operation and which require a detailed investigation to evaluate the underlying causes and determine the necessary corrective measures to ensure the tank's integrity and safety.

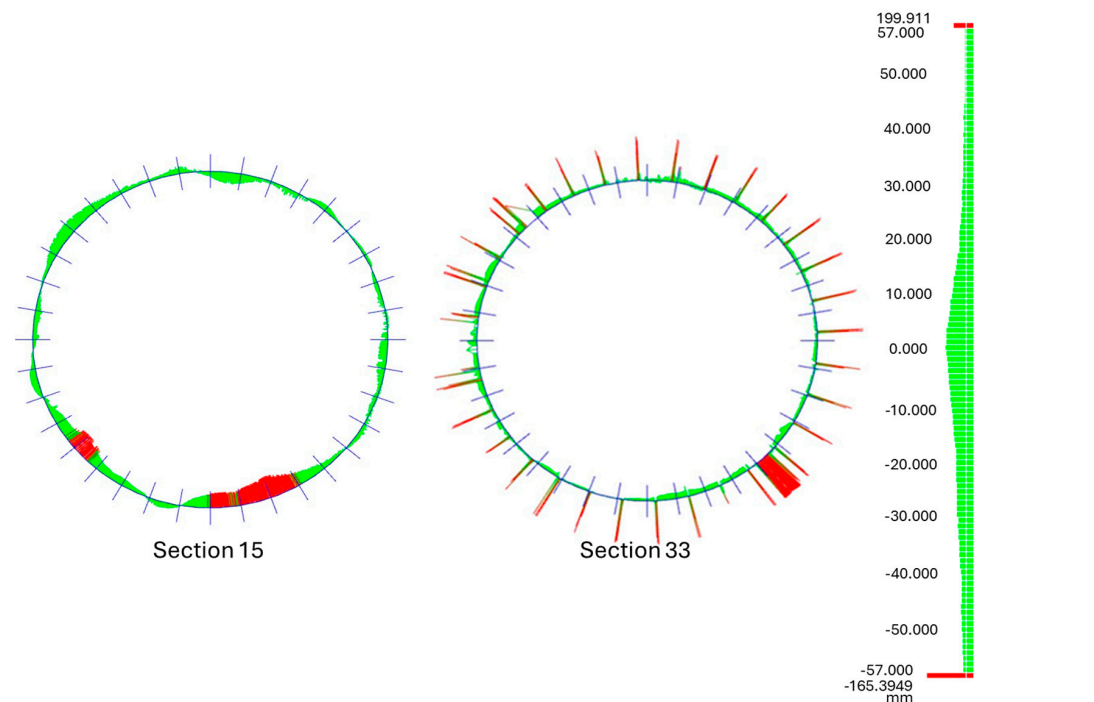


**Figure 8.** Roundness study in sections 15 and 33.

In contrast, horizontal section 33 of the tank, which is located near the tank's base, exhibits better roundness compared to the other sections. This section has the smallest variation between its maximum outward and inward deviations (57.312 mm) and a more uniform distribution of deviations along the circumference. Despite the apparent better roundness of section 33 compared to the other sections, the deviations in this section still surpass the previously mentioned allowable limits ( $\pm 19$  mm) set by the API 653 standard.

The results of this analysis reveal the presence of significant deviations in the roundness of several tank sections. These deviations may have implications for the tank's structural integrity and performance. It is essential to conduct further monitoring and a more detailed evaluation of the identified sections to determine the underlying causes of these deviations and to take the necessary corrective measures to ensure the tank's safety and operational efficiency.

### 3.1.2. Tank Verticality Analysis

According to API 650, the maximum verticality tolerance is set at 1/200 of the total height of the tank. This means that for a tank with a height of 26,320 mm, the allowable verticality deviation would be 131.6 mm. However, API 653 further restricts the verticality tolerance to 1/100 of the tank height, with an absolute maximum limit of 127 mm.

In order to ensure compliance with the most stringent requirements, the verticality analysis of the tank in this study was conducted using the API 653 tolerance of 127 mm. This conservative approach guarantees that the tank's verticality remains within the acceptable limits set by the industry standards.

To conduct a comprehensive assessment of the tank's verticality, all sections of the tank have been analyzed. Table 4 presents the most significant deviations identified in this study.

**Table 4.** Deviations in tank vertical sections.

Sector	Maximum (mm)	Minimum (mm)	Difference (Max-Min) (mm)	Mean
220°	82.094	−28.107	110.201	32.505
130°	19.757	−10.235	29.992	5.131
350°	8.828	−26.831	35.659	−1.645
10°	−24.325	−82.662	58.337	−46.378

The maximum vertical deviation found in the tank is 82.094 mm, which occurs in the 220° column. This value is within the allowable limit specified by the API 653 standard, which sets a maximum verticality tolerance of 127 mm, as discussed in the applicable regulations section.

The 220° sector exhibits the greatest difference between the maximum outward and inward values, with a range of 110.201 mm. This indicates a significant variation in verticality within this sector. In contrast, the 130° sector has the smallest difference between the maximum outward and inward values, with a range of 29.992 mm, suggesting a more consistent verticality profile.

When considering the mean values, the 350° sector has the smallest mean in absolute value at −1.645 mm, indicating a relatively small average deviation from the vertical axis. On the other hand, the 10° sector has the largest absolute mean value of −46.378 mm, suggesting a more pronounced average deviation towards the interior of the tank.

Figure 9 indicates a cut of the tank where sections 40 and 220° are shown. The section at 220° of the tank presents the greatest lack of verticality among all the analyzed columns, with a wide variation between maximum outward and inward deviations (110.201 mm).

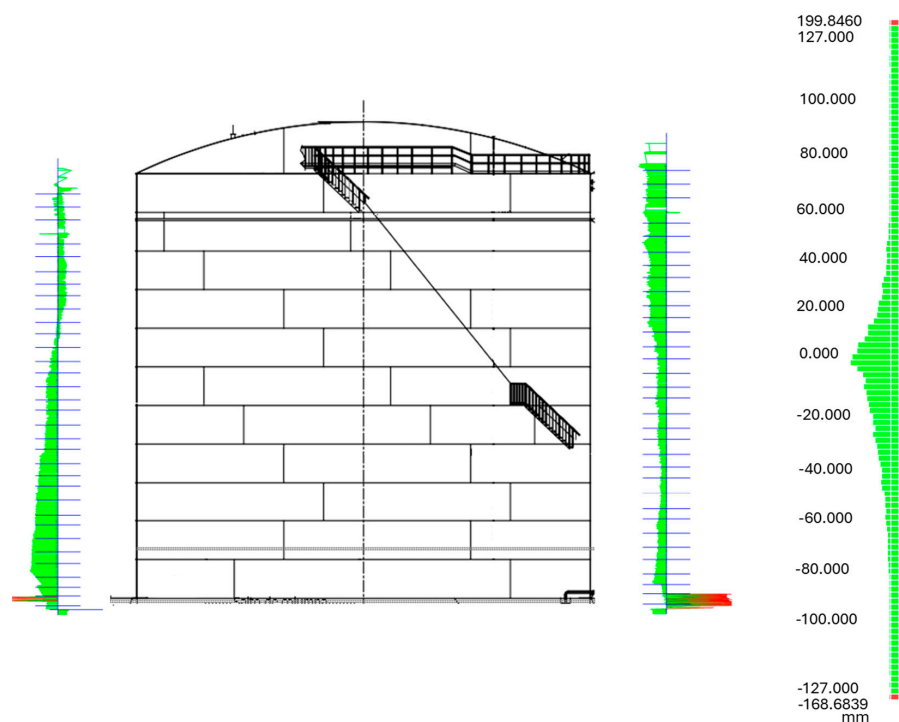


**Figure 9.** Analysis of verticality in the tank cut from 40 to 200 degrees.

The graph shows an asymmetric distribution of deviations along the tank's height, with a clear tendency towards positive deviations at the top (maximum of 82.094 mm) and less pronounced negative deviations at the bottom (minimum of  $-28.107$  mm). This irregular shape suggests verticality problems that could be due to imperfections in construction, uneven loads, ground settlements, or deformations caused by temperature or pressure changes. It is crucial to evaluate the underlying causes and determine if corrective measures are required to ensure the tank's integrity and safety, considering that the red protrusion at the top corresponds to an instrument and should not be interpreted as an actual deviation of the structure.

### 3.1.3. Analysis of Tank Walls

Figure 10 shows a two-dimensional color map representing the unrolled tank walls, allowing for a detailed visualization of the deformations and deviations from verticality across the entire tank surface. This approach provides a comprehensive overview of the tank's structural integrity and facilitates the identification of critical areas that require attention.

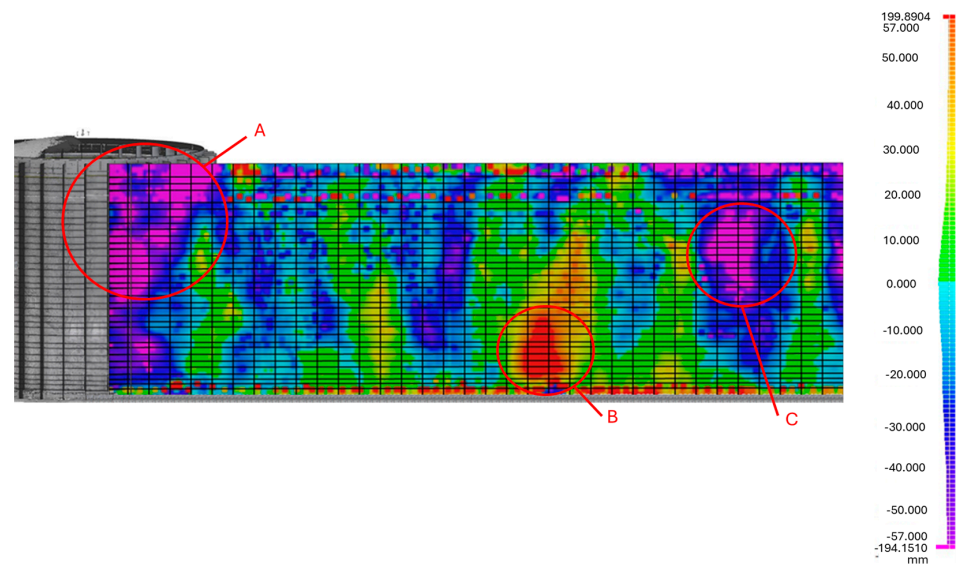


**Figure 10.** Analysis results (2D color map) with referenced sections.

The color map employs a scale ranging from dark blue to intense red to indicate the magnitude and direction of the deformations. Cool colors, such as blues and greens, represent negative or inward deviations in the tank, suggesting the presence of dents or areas where the tank wall is below the ideal surface. On the other hand, warm colors, such as yellows, oranges, and reds, indicate positive or outward deviations, implying the existence of protrusions or areas where the tank wall is above the ideal surface.

In Figure 10, three areas are highlighted by circles representing zones with greater deviations on the tank surface:

- Zone A (Vertical sector:  $0^\circ$  to  $30^\circ$ , Horizontal sector: 1 to 18): Maximum inward deviation of 94.840 mm and an average value in that zone of 35 mm inward deviation.
- Zone B (Vertical sector:  $200^\circ$  to  $220^\circ$ , Horizontal sector: 20 to 33): Maximum outward deviation of 82.094 mm and an average value in that zone of 17.260 mm outward deviation.
- Zone C (Vertical sector:  $300^\circ$  to  $310^\circ$ , Horizontal sector: 5 to 18): Maximum inward deviation of  $-80.802$  mm and an average value in that zone of 80.802 mm inward deviation.

These local deviations may be associated with problems during the assembly or welding process and require special monitoring to prevent the development of failures due to stress concentration.

When interpreting the color map, it is crucial to consider certain aspects to avoid misinterpretations. Firstly, the data above horizontal section 1 can be disregarded, as it corresponds to the region where the shell plate ends and the upper stiffener ring and handrail support are located. These additional structures may generate variations in the data that do not necessarily represent the actual deformations of the tank wall.

Secondly, at a height of 23,520 mm, there is an intermediate stiffener ring (Figure 11), which may also show data that appears to indicate deformations on the color map. However, it is important to recognize that these variations are attributable to the presence of the ring and should not be interpreted as genuine deformations of the tank wall. These images complement the color map and help contextualize the observed variations in those specific regions of the tank.

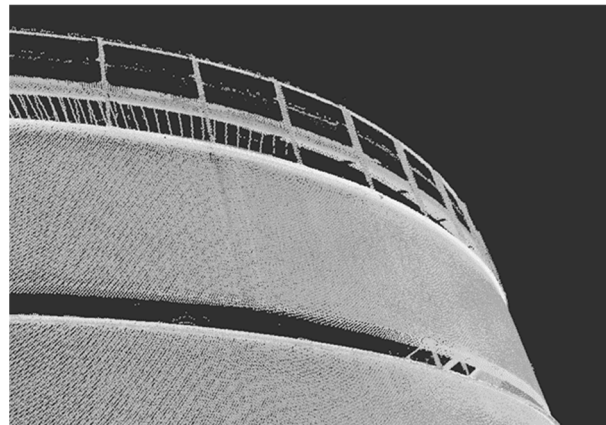


**Figure 11.** Intermediate stiffener ring.

### 3.2. Analysis of Roof Flatness

The roof flatness analysis was performed by comparing the triangular mesh generated by photogrammetry with an ideal horizontal plane using 3DReshaper software.

Figure 12 presents a detailed analysis of the flatness of the tank roof, carried out by comparing a triangular mesh generated by photogrammetry with an ideal horizontal plane using 3DReshaper software.

The results are displayed in the form of a heat map, where the color scale represents height deviations from the reference plane. Blue tones indicate the lowest areas, with a minimum elevation of 0.915 m at point 2, while red tones indicate the highest areas, reaching a maximum elevation of 1.069 m at point 1. Therefore, the maximum height difference between the highest and lowest points of the roof is 154 mm, representing the maximum unevenness present on the tank roof surface. The legend also provides information on the percentage of values corresponding to each elevation range.

The heat map reveals a heterogeneous color distribution, indicating significant variations in surface elevation. Most of the roof presents green and yellow tones, suggesting an intermediate elevation range. However, localized blue and red areas are also noticeable, indicating the presence of lower and higher zones, respectively.

The color distribution is neither uniform nor symmetrical, implying that the roof is not completely flat. Irregular patterns and abrupt color changes are observed, especially near the center and towards the edges of the image, suggesting the existence of unevenness, protrusions, or depressions in certain areas of the surface.

Therefore, the visual analysis of the heat map reveals considerable irregularities in the flatness of the tank roof. The heterogeneous color distribution and the observed unevenness indicate that the surface is not completely flat and has significant height variations. This flatness analysis, based on photogrammetric techniques and visualization through heat maps, provides a valuable tool to evaluate the construction quality and structural integrity of the roof, allowing the identification of areas that may require attention or repairs to ensure optimal and safe performance.

A detailed visual inspection and periodic monitoring are recommended to assess their evolution over time and prevent failures due to fatigue or collapse.

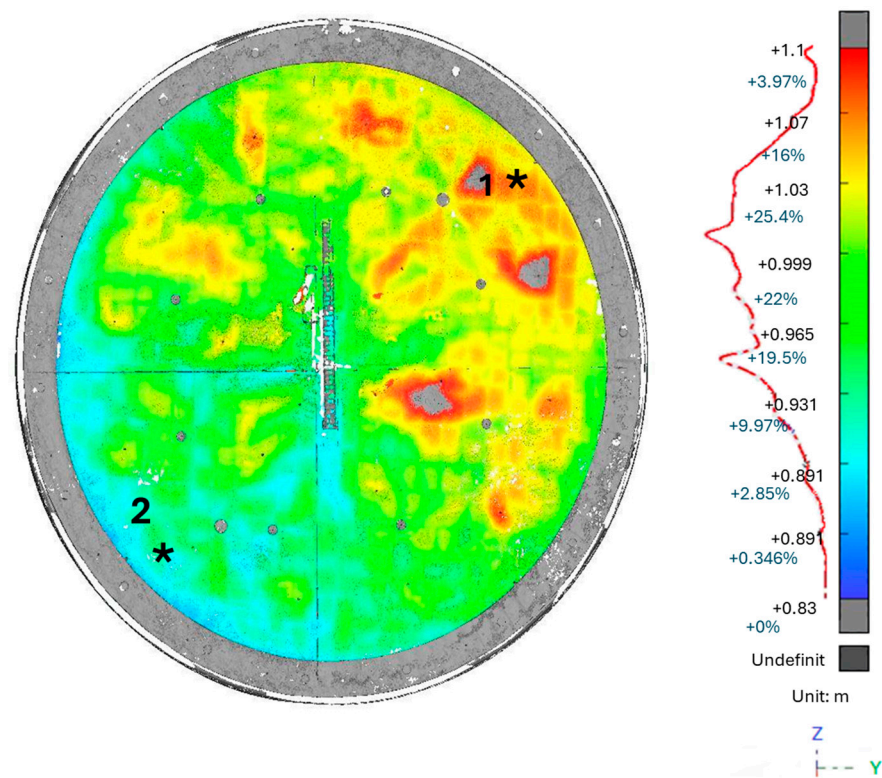


**Figure 12.** Roof flatness in heat map.

#### 4. Discussion

The present study has demonstrated the feasibility and usefulness of the combined application of TLS technology and UAS photogrammetry techniques to perform a detailed and accurate dimensional analysis of a large storage tank. The results obtained have made it possible to identify, quantify, and evaluate significant geometric deviations in the verticality and roundness of the shell, as well as in the flatness of the roof, in relation to the tolerances established by the API 650 and API 653 standards.

The analysis of the tank shell revealed significant inward and outward deviations from the reference dimensions. The presence of these deviations could have a considerable impact on the tank's structural integrity and may require corrective measures. The identified critical sections, such as sections 15 and 27, exhibit a notable lack of roundness, with differences between the maximum outward and inward deviation values exceeding 135 mm. Several sections were found to be outside the allowed values. These deviations can be indicative of problems during construction, uneven loads, ground settlements, or accumulated damage during operation.

Furthermore, the verticality analysis showed that the section at 220° presents the greatest lack of verticality, with a wide variation between the maximum outward and inward deviations of 110.201 mm. Although this deviation falls within the limits allowed by the API 653 standard, it is crucial to investigate the underlying causes and consider corrective measures to prevent the further deterioration of the structure.

The two-dimensional color map generated from the tank's point cloud allowed for a clear visualization of the deviations across the entire surface. This approach facilitates the identification of critical areas and provides a solid foundation for informed decision making regarding tank maintenance and repair.

The flatness analysis of the tank roof, performed by comparing a photogrammetrically generated triangular mesh with an ideal horizontal plane using 3DReshaper software,



reveals significant irregularities in the roof's surface. The non-uniform and asymmetrical color distribution suggests the presence of unevenness, protrusions, and depressions across the roof surface. This analysis highlights the importance of utilizing photogrammetric techniques and heat map visualization as valuable tools for assessing the construction quality and structural integrity of the roof. The findings underscore the need for detailed visual inspections and periodic monitoring to track the evolution of these irregularities over time and prevent potential failures due to fatigue or collapse.

These findings are consistent with previous studies that have used 3D measurement techniques for the inspection and evaluation of storage tanks. For example, ref. [1] applied TLS technology to generate high-resolution 3D models of a cylindrical oil tank and detect deformations in its shell. Similarly, ref. [16] used UAS photogrammetry to generate 3D models of port infrastructure, including storage tanks, and integrate them with BIM (building information modeling) for facility management.

Furthermore, other recent studies have demonstrated the effectiveness of 3D measurement techniques for the inspection of different types of industrial structures, such as bridges [7], pipelines [8], and wind turbine blades [4], highlighting their ability to capture detailed and accurate information quickly and safely.

However, unlike these previous studies, which mainly focused on the generation of geometric models and the qualitative detection of anomalies, the present study has gone one step further by performing a detailed quantitative analysis of deviations from normative tolerances and by investigating the patterns and possible causes of these deviations.

In particular, the analysis of the distribution of verticality deviations along the height of the tank has revealed a clear trend of deviations increasing in magnitude and dispersion towards the base of the tank, as well as a change in the shape of the distribution, going from being skewed to the left and flatter than normal at the top, to being skewed to the right and more pointed than normal at the bottom. This trend is consistent with the expected effect of the accumulation of loads and stresses towards the base of the tank due to the weight of the stored product and the interaction with the foundation [2].

These results agree with those obtained by the authors of [3], who investigated the effect of multi-hazard scenarios on the structural response of atmospheric storage tanks through a simplified methodology, finding that the combination of different loads, such as wind, seismic, and thermal loads, can significantly affect the stress distribution and deformation patterns of the tank, especially in the lower part of the shell.

On the other hand, the correlation analysis between the verticality and roundness deviations showed an increasing relationship between both variables as one descends towards the base of the tank, which suggests that the deformations in this area may be influenced by a common mechanism, such as instability due to buckling or local plasticization of the material due to stress concentration [2].

These results are consistent with those reported by other authors who have recently investigated the structural behavior of storage tanks using advanced numerical modeling and simulation techniques. For example, ref. [8] proposed a methodology for the safety assessment of vertical storage tanks based on online ultrasonic inspection with robots, which allows for detecting and characterizing local defects and deformations in the tank wall. Their results showed that the presence of geometric imperfections, such as out-of-roundness or local buckling, can significantly affect the stress distribution and the risk of failure of the tank, especially when subjected to dynamic loads or extreme operating conditions.

Similarly, ref. [7] developed an automatic damage detection system for concrete bridges based on UAV (unmanned aerial vehicle) remote sensing and deep learning techniques that allows for identifying and classifying different types of surface defects, such as cracks, spalling, or corrosion, from high-resolution images captured by drones. Their approach demonstrated high accuracy and efficiency in detecting and quantifying damage, even in large and complex structures, which could be extended to the inspection of storage tanks and other industrial facilities.

The results of the present study have also highlighted the importance of integrating data obtained through 3D measurement techniques with other sources of information relevant to the evaluation of the structural integrity of storage tanks, such as the history of previous inspections and repairs, process and operating conditions data, as well as the results of numerical modeling and risk analysis.

This multidisciplinary and multi-source integration is consistent with the recommendations of various authors and international organizations that have recently addressed the management of the integrity of industrial assets. For example, the [20] standard on the risk-based inspection of pressure equipment emphasizes the need to use a comprehensive and systematic approach to assess the probability and consequences of equipment failure, considering both the data obtained through inspection and monitoring techniques as well as the information derived from process safety management, mechanical integrity programs, and asset reliability strategies.

Similarly, the [21] standard on the collection and exchange of reliability and maintenance data for equipment in the petroleum, petrochemical, and natural gas industries highlights the importance of establishing a standardized and consistent data management system that allows for the integration of information from different sources and stages of the asset life cycle, such as the design, operation, inspection, maintenance, and decommissioning stages. This standard provides guidelines and principles for the definition of data categories, quality requirements, exchange formats, and analysis methods that can be applied to the management of the inspection data from storage tanks and other critical equipment.

Another relevant aspect to discuss is the potential impact of 3D measurement techniques on the safety and efficiency of storage tank inspection and maintenance operations. Traditionally, these operations have required direct access to the structure by personnel, whether using scaffolding, elevated platforms, or rope access techniques, which carries risks of falling, entrapment, or exposure to hazardous substances [6].

In this sense, the application of TLS technology and photogrammetry techniques with drones can help reduce the need for direct access and, therefore, minimize the risks for the personnel involved in inspections [16]. Furthermore, these techniques allow a large amount of data to be captured in a relatively short time and without interrupting normal tank operations, which can translate into significant savings in terms of time and costs [9].

These advantages have been recognized by various authors, such as those from [22], who carried out a comparative analysis between traditional tank inspection techniques and drone-based techniques, highlighting the benefits of the latter in terms of safety, efficiency, and quality of the data obtained. Their results suggest that drone inspection can reduce the inspection time by up to 80% and the associated costs by 60%, while improving personnel safety and the completeness and accuracy of the information captured.

However, it is important to recognize that the effective implementation of these techniques requires properly trained and qualified personnel, both for the operation of the measurement equipment and for the processing and analysis of the data obtained [18]. In addition, clear protocols and procedures must be established to guarantee the quality, security, and consistency of the results, as well as for the proper management and storage of the generated information [17].

In this context, [23] proposed a methodology for the use of 360-degree panoramic images of reality (PARS) for construction safety training, which allows workers to visualize and interact with realistic representations of the work environment, including potential hazards and safe practices. This approach could be extended to the training of personnel involved in tank inspection activities, using immersive virtual reality techniques based on TLS technology and photogrammetry data.

It is also necessary to consider the limitations and technical challenges associated with the application of 3D measurement techniques in complex and large-scale industrial environments. For example, the presence of obstacles, vegetation, or adverse weather conditions can affect the quality and completeness of the captured data, requiring advanced

processing and filtering techniques for its purification and analysis [10]. Likewise, integrating and accurately georeferencing multiple point clouds or 3D models can be challenging, especially in large structures or those with complex geometries [5].

These limitations have been addressed by various authors, such as those from [24], who developed a methodology for the automatic detection of disaster damage in buildings using deep learning techniques and 3D point cloud features derived from oblique aerial images. Their approach allows for identifying and classifying different types of structural damage, such as cracks, spalling, or collapses, in a fast and accurate way, even in the presence of occlusions, clutter, or variable lighting conditions.

Similarly, ref. [25] proposed a methodology for the degradation modeling and maintenance planning of railway track geometry using 3D laser scanning data and machine learning techniques. Their approach allows for characterizing the evolution of track geometry defects over time, considering different influencing factors, such as traffic, environmental conditions, or maintenance actions, and optimizing inspection and repair strategies based on risk and cost–benefit criteria.

Another important challenge is the effective management and exploitation of the large volume of data generated by 3D measurement techniques, which may require specialized storage and processing infrastructure, as well as advanced visualization and analysis tools [18]. In this sense, the development and application of artificial intelligence and machine learning techniques can be very useful to automate and optimize the processing and extraction of relevant information from the captured data [4].

In this regard, ref. [4] proposed a methodology for the automatic detection of multi-type surface defects in wind turbine blades using a cascade deep learning network and high-resolution images captured by drones. Their approach allows for identifying and classifying different types of defects, such as cracks, erosion, delamination, or lightning strikes, with an accuracy greater than 90%, significantly reducing the time and cost of blade inspection compared to manual methods.

In conclusion, the present study has demonstrated the potential of 3D measurement techniques, such as TLS technology and UAS photogrammetry, to improve the efficiency, safety, and reliability of storage tank inspection and assessment operations. The results obtained have made it possible to identify and quantify significant geometric deviations in a real case study, as well as analyze their possible causes and consequences for the structural integrity of the tank.

Although some limitations and technical challenges associated with the application of these techniques in complex industrial environments have been identified, it is considered that their potential benefits far outweigh their possible drawbacks, as long as they are implemented appropriately and integrated into a comprehensive and risk-based asset management system.

To make the most of the potential of these techniques, it is necessary to continue researching and developing new methodologies and standards that allow for addressing the identified challenges, as well as promoting multidisciplinary collaboration between experts in different areas, such as structural engineering, metrology, computer science, and asset management.

Only in this way can we move towards smarter, safer, and more sustainable management of critical industrial assets, such as storage tanks, contributing to the development and well-being of society as a whole.

## 5. Conclusions

The present work has demonstrated the successful application of advanced TLS technology and UAS photogrammetry techniques to perform a detailed and accurate dimensional analysis of a large storage tank. The results obtained have made it possible to identify, quantify, and evaluate significant geometric deviations in the verticality and roundness of the shell, as well as in the flatness of the roof, in relation to the tolerances established by API 650 and API 653 standards.

The methodology used, based on the capture of high-density and precision point clouds through TLS technology and photogrammetry, has proven to be an efficient and reliable alternative to traditional manual inspection and measurement methods, which are usually slower, more expensive, and riskier for the personnel involved. The generation of complete and detailed three-dimensional models of the tank has made it possible to carry out an exhaustive analysis of its geometry and detect deviations and anomalies that could go unnoticed with conventional techniques.

Furthermore, the integration of TLS technology and photogrammetry data into a single consolidated model has facilitated the comparison and validation of the results obtained by both techniques, increasing the reliability and robustness of the analysis. The application of advanced point cloud processing and visualization tools, such as segmentation, generation of sections, and comparison with ideal models, has allowed valuable information to be extracted about the patterns and distribution of geometric deviations throughout the structure.

The results of the analysis have revealed the presence of significant deviations in the verticality of the shell, with values that exceed regulatory tolerances in several areas, especially in the lower part of the tank. These deviations present a pattern of increase and concentration towards the base, which suggests the influence of factors such as the accumulation of loads and stresses due to the weight of the stored product and the interaction with the foundations. Furthermore, an increasing correlation was found between the verticality and roundness deviations as one descends towards the base, which indicates the possible existence of common deformation mechanisms, such as instability due to buckling or local plasticization of the material.

The flatness analysis of the tank roof using photogrammetry and 3D visualization software reveals significant surface irregularities, highlighting the importance of these techniques for assessing roof construction quality and structural integrity. These anomalies may be related to design, manufacturing, or roof deterioration problems and may have a negative impact on the safety and operation of the tank by favoring the accumulation of water, corrosion, and the concentration of stress in the affected areas.

These findings highlight the importance of conducting regular and detailed inspections of storage tanks to detect and evaluate possible geometric deviations that may compromise their long-term structural integrity and functionality. The application of advanced three-dimensional measurement techniques, such as TLS technology and photogrammetry, can significantly improve the efficiency, safety, and reliability of these inspections by providing objective, complete, and accurate information on the true state of the structure.

However, it is important to recognize that these techniques do not completely replace other inspection and evaluation methods but rather complement and enhance them. To obtain a comprehensive understanding of the condition and behavior of storage tanks, it is necessary to integrate the geometric data obtained through TLS technology and photogrammetry with additional information, such as the history of previous inspections and repairs, process data and operating conditions, results of non-destructive testing, and structural and risk analyses.

This multidisciplinary and multi-source integration is essential to develop effective tank integrity and maintenance management strategies that optimize their performance, prolong their useful life, and ensure their long-term safety and reliability. To achieve this, it is necessary to establish frameworks and methodologies that facilitate the capture, processing, analysis, and decision making based on data, taking advantage of emerging technologies such as the Internet of Things, artificial intelligence, and augmented reality.

Furthermore, it is essential to foster collaboration and knowledge exchange between the different actors involved in the management of storage tanks, including operators, inspectors, engineers, researchers, and regulators. Only through a multidisciplinary and collaborative approach can the technical, operational, and regulatory challenges associated with the inspection and evaluation of these critical assets be effectively addressed.

In this sense, the present study contributes to advancing the knowledge and application of advanced three-dimensional measurement techniques for the inspection and analysis of storage tanks, laying the foundations for the development of future research and applications in this field. Some of the aspects that will require further attention and development in the future include:

- The standardization and normalization of procedures for capturing, processing, and analyzing laser scanning and photogrammetry data to ensure the quality, consistency, and interoperability of the results obtained by different equipment and in different operational contexts.
- The development of intelligent point cloud analysis algorithms and tools based on machine learning and computer vision techniques that allow for automating and optimizing the detection, classification, and quantification of anomalies and defects in the inspected structures, reducing subjectivity and human error.
- The integration of three-dimensional inspection data with other technical information, maintenance, and asset integrity management systems, such as condition monitoring systems, finite element models, or digital twins, to facilitate informed and optimized decision making on repair, replacement, or life extension actions for critical components.
- The education and training of specialized personnel in the operation and analysis of TLS technology and photogrammetry data, as well as in its integration with other disciplines and tools of maintenance and reliability engineering, to ensure the quality and efficiency of inspections and evaluations carried out.

In conclusion, the application of TLS technology and UAS photogrammetry techniques for the dimensional analysis of storage tanks presents a valuable opportunity to improve the safety, reliability, and efficiency of these critical assets by providing detailed, accurate, and objective information about their geometric and structural state. However, to take full advantage of the potential of these techniques, it is necessary to continue researching and developing new methodologies and standards to address the technical, operational, and regulatory challenges associated with their implementation in complex industrial environments.

Only through a multidisciplinary, collaborative, and data-driven approach can we move towards smarter, safer, and more sustainable management of storage tanks and other critical industrial assets, thus contributing to the development and well-being of society as a whole. The present work represents an important step in that direction by demonstrating the feasibility and benefits of applying advanced three-dimensional measurement techniques for the inspection and analysis of these structures and by identifying opportunities and challenges that will need to be addressed in the future to consolidate and extend their use in the industry.

**Author Contributions:** Conceptualization, S.G.-M., P.G.-T., A.S.-C., A.G.-G. and F.H.-C.; methodology, S.G.-M. and A.G.-G.; software, S.G.-M., P.G.-T. and A.S.-C.; validation, S.G.-M., P.G.-T. and A.S.-C.; formal analysis, A.G.-G.; investigation, A.G.-G. and F.H.-C.; resources, S.G.-M., P.G.-T. and A.S.-C.; data curation, S.G.-M., P.G.-T. and A.S.-C.; writing—original draft preparation, A.G.-G. and F.H.-C.; writing—review and editing, A.G.-G. and F.H.-C.; visualization, A.G.-G. and F.H.-C.; supervision, S.G.-M., P.G.-T. and A.S.-C.; project administration, P.G.-T. and A.S.-C.; funding acquisition, P.G.-T. and A.S.-C. All authors have read and agreed to the published version of the manuscript.

**Funding:** This research received no external funding.

**Data Availability Statement:** Data are contained within the article.

**Acknowledgments:** The authors also thank the editor and anonymous reviewers for their valuable advice.

**Conflicts of Interest:** The authors declare no conflicts of interest.



## References

1. Li, J.; Lv, W. The Research Application of 3D Laser Scanning Technology in the Deformation Detection of Large Cylindrical Oil Tank. *J. Archit. Res. Dev.* **2022**, *6*, 14–20. [\[CrossRef\]](#)
2. Paz, J.; Robles, C.; Cheng, F. Buckling of aboveground storage tanks: A state-of-the-art review. *Thin-Walled Struct.* **2021**, *167*, 108193. [\[CrossRef\]](#)
3. Wang, J.; Weng, W. A Simplified Methodology for Rapidly Analyzing the Effect of Multi-Hazard Scenario on Atmospheric Storage Tanks. *Preprint* **2021**. [\[CrossRef\]](#)
4. Mao, Y.; Wang, S.; Yu, D.; Zhao, J. Automatic image detection of multi-type surface defects on wind turbine blades based on cascade deep learning network. *Intell. Data Anal.* **2021**, *25*, 463–482. [\[CrossRef\]](#)
5. Wang, Q.; Kim, M.K.; Cheng, J.C.; Sohn, H. Automated quality assessment of precast concrete elements with geometry irregularities using terrestrial laser scanning. *Autom. Constr.* **2019**, *108*, 102978. [\[CrossRef\]](#)
6. Gálvez, P.; Pereira, M.; Silva, A.R.; Fonseca, F.; Ferreira, A.; de Brito, J. Acoustic emission monitoring of existing steel storage tanks. *J. Constr. Steel Res.* **2021**, *183*, 106713.
7. Liang, H.; Lee, S.-C.; Seo, S. UAV-Based Low Altitude Remote Sensing for Concrete Bridge Multi-Category Damage Automatic Detection System. *Drones* **2023**, *7*, 386. [\[CrossRef\]](#)
8. He, L.; Wu, J.; Wang, X.; Kang, Y.; Huang, Z.; Wang, H.; Wang, W. Safety Assessment of Vertical Storage Tank Based on Robot Ultrasonic Online Inspection. *J. Nondestruct. Eval.* **2023**, *42*, 29. [\[CrossRef\]](#)
9. Jiang, S.; Jiang, W.; Huang, W.; Yang, L. UAV-based oblique photogrammetry for outdoor data acquisition and offsite visual inspection of transmission line. *Remote Sens.* **2019**, *11*, 278. [\[CrossRef\]](#)
10. Dong, Z.; Liu, S.; Luo, X. Point cloud analysis for automated inspection of industrial structures: A survey. *Sensors* **2021**, *21*, 5136. [\[CrossRef\]](#) [\[PubMed\]](#)
11. Lopes, M.A.; Soeiro, F.J.; Silva, J.G.S. Nonlinear buckling behavior and stress and strain analyses of atmospheric storage tank aided by laser scan dimensional inspection technique. *J. Braz. Soc. Mech. Sci. Eng.* **2022**, *44*, 443. [\[CrossRef\]](#)
12. Tao, X.; Zhang, L.; Li, J. Automated surface defect detection for mobile phone screen glass based on deep learning. *Sensors* **2020**, *20*, 5212. [\[CrossRef\]](#) [\[PubMed\]](#)
13. Truong-Hong, L.; Lindenbergh, R.; Fisk, P. Storage Tank Inspection Based Laser Scanning. In *Lecture Notes in Civil Engineering*; Springer: Singapore, 2020; Volume 56, pp. 996–1005. [\[CrossRef\]](#)
14. Akbari, H.; Sadeghi, S.H.; Loghavi, M. Application of UAV photogrammetry for estimating soil surface roughness. *Int. Agrophys.* **2021**, *35*, 1–13.
15. Jiang, S.; Jiang, W.; Wang, L. Unmanned Aerial Vehicle-Based Photogrammetric 3D Mapping: A survey of techniques, applications, and challenges. *IEEE Geosci. Remote Sens. Mag.* **2021**, *10*, 135–171. [\[CrossRef\]](#)
16. Jofré-Briceño, C.; Muñoz-La Rivera, F.; Atencio, E.; Herrera, R.F. Implementation of Facility Management for Port Infrastructure Using UAVs, Photogrammetry and BIM. *Sensors* **2021**, *21*, 6686. [\[CrossRef\]](#) [\[PubMed\]](#)
17. Kumar, S.A.; Ilango, P.; Antony Venus, A.J. Structural Health Monitoring of Storage Tanks Using Drone-Based 3D Scanning Techniques. In *Advances in Structural Engineering*; Springer: Singapore, 2021; pp. 229–241. [\[CrossRef\]](#)
18. Lv, S.; Zhang, H.; Bao, F. Health Management Control Strategy of Tank Storage Based on Artificial Intelligence. In Proceedings of the 2020 IEEE 3rd International Conference on Automation, Electronics and Electrical Engineering (AUTEEE), Shenyang, China, 20–22 November 2020; pp. 91–95. [\[CrossRef\]](#)
19. Singh, P.; Sathiyasekar, A.; Prabhakaran, R.R.; Jessy, C.J.; Pushpagiri, J. Automated defect detection in storage tanks using a magnetic flux leakage robot. *J. Nondestruct. Eval.* **2021**, *40*, 39. [\[CrossRef\]](#)
20. *API RP 581*; Risk-Based Inspection Methodology. American Petroleum Institute: Washington, DC, USA, 2022.
21. *ISO 14224:2022*; Collection and Exchange of Reliability and Maintenance Data for Equipment in the Petroleum, Petrochemical and Natural Gas Industries. International Organization for Standardization: Geneva, Switzerland, 2022.
22. Ruggiero, A.; Galli, G.; Carcagni, P.; De Fazio, R.; Tati, A.; Boschetto, C.; Galiano, G. Photogrammetric survey for the retrofitting and restoration of industrial archaeology: The case of the De Cecco company grain silos (Pescara, Italy). *Appl. Geomat.* **2020**, *12*, 579–586. [\[CrossRef\]](#)
23. Habib, M.; Alzubi, Y.; Malkawi, A.; Awwad, M. Impact of artificial intelligence on construction safety: A review. In Proceedings of the 2020 IEEE 6th International Conference on Control Science and Systems Engineering (ICCSSE), Beijing, China, 17–19 December 2020; pp. 150–155. [\[CrossRef\]](#)
24. Czerniawski, T.; Leite, F. Automated building change detection with amodal completion of point clouds. *Autom. Constr.* **2020**, *118*, 103306. [\[CrossRef\]](#)
25. Qian, X.; Jia, D. A survey on track geometry degradation modelling and monitoring technologies: From theory to practice. *Measurement* **2021**, *184*, 109915.

**Disclaimer/Publisher’s Note:** The statements, opinions and data contained in all publications are solely those of the individual author(s) and contributor(s) and not of MDPI and/or the editor(s). MDPI and/or the editor(s) disclaim responsibility for any injury to people or property resulting from any ideas, methods, instructions or products referred to in the content.